Lensing effects on gravitational waves from compact binaries

Author: Helena Ubach Raya
Facultat de Física, Universitat de Barcelona, Diagonal 645, 08028 Barcelona, Spain.

Advisor: Oleg Bulashenko

Abstract: Compact binary systems, such as black holes or neutron stars, are known to emit gravitational waves as a result of energy loss while orbiting around their common center of mass. Ground-based detectors like LIGO and VIRGO have been able to detect such radiation as a "chirp" signal in the range of frequencies emitted by these compact systems. It is known that gravitational waves can experience gravitational lensing as they travel from the binary system to the observer and pass near massive objects on their way. This produces a distortion which could be encoded in the signal we detect. In this work we analyse wave effects on gravitational lensing of gravitational waves (like interference and diffraction) which are of possible importance in future detections by ground-based and/or space detectors.

I. INTRODUCTION

Gravitational waves (GWs) are disturbances of space-time curvature produced by moving masses. Their effect is extremely small, so only those created where the space-time is greatly distorted can be detected today. One of this cases, the one we will use for our studies, is binary mergers: pairs of compact objects - black holes (BH) or neutron stars (NS) - that orbit each other. They get closer together by losing energy in form of GWs, until they merge, creating a new compact remnant. The detectable GWs are those generated just before and after the merger. There are three phases: inspiral, merger and ringdown. We will center in the inspiral phase.

These waves can be affected by the space-time curvature created by masses along their way, and they get distorted (gravitationally lensed); the intervening mass is then called a gravitational lens.

Historically, gravitational lenses had first been treated in the electromagnetic case (light). This should only be possible by taking into account that light has inertia: the first to write about the attraction of light due to gravity was Isaac Newton in his book *Opticks*, imagining that light was corpuscular [1]. Later, other scientists calculated the Newtonian value of the deflection of light by a mass (Cavendish, Soldner). However, the theory of gravity was not yet complete: in 1915 the theory of General Relativity derived by Albert Einstein predicted twice the Newtonian value, and the result was confirmed by observations of the star position deviations during a solar eclipse in 1919 (led by Arthur Eddington). From that moment on, more investigations on this phenomenon were made, and it was discovered that multiple images of the same object can be seen when light is bent by gravity, and that their luminosity can vary from its original value. Eventually, this has been called gravitational lensing.

Recently, gravitational lensing of GWs has also been taken into consideration in theoretical calculations, but not as much as light. Now that GWs have been detected with interferometers for the first time, more attention is being paid to them.

In this work, we will first discuss the characteristic profile of pure (unlensed) GWs generated by binary mergers, called "chirp" in Sec. II. Then, we describe how GWs get lensed in Sec. III, and apply the results for a particular lens model, the *point mass lens* in Sec. IV. Then, in Sec. V we study the so called amplification factor, which is a measure of the wave amplitude distortion due to the gravitational lensing. Finally, in Sec. VI we review the most important aspects of the work, that wave effects are important, and possible future improvements.

II. CHIRP

In the inspiral phase, just before the merger, the gravitational waves coming from the binary system increase in frequency, as a result of an increasing orbital frequency (since it is quadrupolar radiation, the gravitational wave frequency is double that of the orbital motion: $f_{GW}(t) = 2f_{orb}(t)$). This increasing frequency is called "chirp" (all the signal, including the inspiral), refering to the similarity with bird chirps. The chirp is shown in Fig. 1 (This and all other figures in this work are processed by Python.)

From the quadrupolar moment tensor one can obtain the power radiated by the binary system [2] and from this, the GWs frequency variation with time [3]:

$$\frac{df_{GW}}{dt} = \frac{96\pi^{8/3}}{5}\left(\frac{GM_c}{c^3}\right)^{5/3} f_{GW}^{11/3}, \qquad (1)$$

where G is the gravitation constant, c the speed of light in vacuum, $M_c \equiv (m_1 m_2)^{3/5}/(m_1+m_2)^{1/5}$ is defined as the *chirp mass*, and m_1, m_2 are the masses of the binary system components. Solving for f_{GW}, we get

$$f_{GW}(t) = \frac{1}{\pi}\left(\frac{5}{256}\frac{1}{(\tau_c - t)}\right)^{3/8}\left(\frac{c^3}{GM_c}\right)^{5/8}, \qquad (2)$$

where τ_c is called coalescence time.

The strain $h(t) = h_0 \cos\phi$ is the instant amplitude of the wave (with h_0 the maximum amplitude and ϕ the

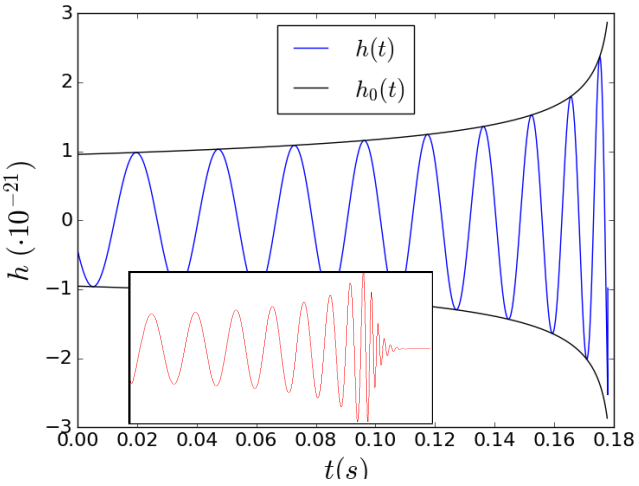

FIG. 1: Strain function $h(t)$ versus t during the inspiral phase of a chirp signal from a stellar-mass binary system. We have taken the GW150914 event parameters as a realistic example. We can see that the h_0 increases as $h_0 \propto f_{GW}^{2/3} \propto (\tau_c - t)^{-1/4}$. It is the first part of the full chirp (little image below, Credit: E. Schnetter et al., "Astrophysical Applications of Numerical Relativity - from Teragrid to Petascale"(2008)).

wave's phase), which coincides with the relative length compression which GWs produce when they pass through an interferometer: $\Delta L/L$, where L is the total object's length. It can have two polarisations, $h_\times$ and h_+, but we use a generalised h_0 (it could be any of both polarisations, or a mix). The expressions for $h_0(t)$ and $\phi(t)$ are [3]

$$h_0(t) = 2\eta^{3/5}\left(\frac{R_S}{d_S}\right)\left(\frac{GM_c\pi}{c^3}f_{GW}(t)\right)^{2/3}, \qquad (3)$$

$$\phi(t) = -2\left(\frac{5GM_c}{c^3}\right)^{-5/8}(\tau_c - t)^{5/8} + \phi_0, \qquad (4)$$

where $\eta = m_1m_2/(m_1+m_2)^2$ is the asymmetric mass, $R_S = 2G(m_1+m_2)/c^2$ is the Schwarzschild radius of the system, d_S is the distance from the observer to the source and ϕ_0 is the initial phase of the GWs in real space. To see easier the frequencies involved in the chirp, it's better to move to the frequency domain, so we will have to Fourier-transform $h(t)$ into $\tilde{h}(f)$, with f being the Fourier variable. It is not possible to make an exact Fourier transform, so we will proceed numerically (using a fast Fourier transform, FFT). However, we would like to have an analytical expression as close to the numerical result as possible, so we will try to solve the Fourier transform integral with approximations.

A. Stationary Phase Approximation

Stationary phase approximation (SPA) consists in considering that most of the contribution to an integral of an oscillating function comes from a stationary point. In our case the integral is the Fourier transform given by [4]

$$\tilde{h}(f) = \int_{-\infty}^{\infty} h(t)e^{i2\pi ft}dt, \qquad (5)$$

with $h(t) = h_0(t)\cos\phi(t)$, from equations (3),(4) being the detector's response function. Following [4], one gets the approximation of $|\tilde{h}(f)|$ (we are interested in the modulus for now):

$$|\tilde{h}(f)| = \frac{h_0(t_f)}{2\sqrt{\dot{f}(t_f)}}, \qquad (6)$$

where t_f is the stationary point, which depends on f, and $\dot{f}(t_f)$ is the time derivative of f. It turns out that the stationary point corresponds to the condition that $f_{GW}(t_f) = f$. With this equality, we can use (1) to obtain the following equation dependent on f:

$$|\tilde{h}(f)| = \sqrt{\frac{5}{96\pi}}\eta^{3/5}\left(\frac{R_S}{d_S}\right)\left(\frac{c^3}{GM_c\pi}\right)^{1/6} f^{-7/6}. \qquad (7)$$

In Fig. 2 we compare the numerical FFT with the SPA

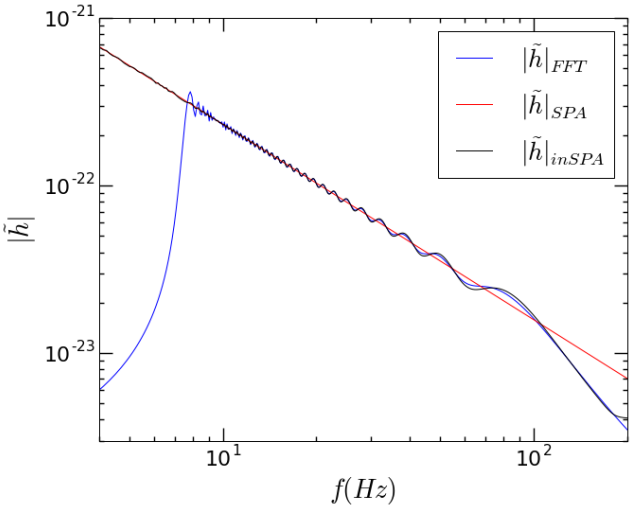

FIG. 2: Detection response function $|\tilde{h}|$ versus f (Fourier space). The exact Fourier transform is plotted in blue. The red line is the usual SPA $|\tilde{h}| \sim f^{-7/6}$, the black one is the improved SPA, $\tilde{h}^{inSPA}$.

approximation. It is seen that the SPA (in red) has the same slope as the FFT (in blue). The curve follows the SPA slope $\tilde{h} \sim f^{-7/6}$. It does not have, however, the oscillations appearing in the FFT result. If we want to have an analytical expression for them, we have to go beyond SPA. Damour et al.[4] have obtained an analytical expression for this oscillations: it is possible to improve the SPA by taking into account border (finite time) effects (we haven't taken an infinite time interval like Eq.

(5)). We compare $\tilde{h}^{inSPA}$ with the numerical FFT result in Fig. 2, where we can see it can fit quite well the oscillations.

III. GRAVITATIONAL LENSING OF GRAVITATIONAL WAVES

Gravitational waves, as well as electromagnetic waves, can be deflected by the space-time curvature. There are some cases when a mass distribution is able to make rays deflect very much like a lens, this mass is then called a gravitational lens (although there are some differences with respect to optical lenses).

If we want to know if wave effects will be important in an electromagnetic or a gravitational wave, we have to compare its wavelength λ with the Schwarzschild radius $R_S = 2GM_L/c^2$, where M_L is the lens' mass. If $\lambda \gg R_S$, then the wave doesn't notice the mass and isn't distorted. In the opposite limit, when $\lambda \ll R_S$, there is gravitational lensing in the Geometrical Optics (GO) limit. An intermediate case which is of our interest is when diffraction and other interference phenomena are important: that happens when $\lambda \gtrsim R_S$. This corresponds to a lens' mass that satisfies $M_L \lesssim 10^5 (M_\odot/f)$ Hz (where $M_\odot$ is the solar mass and f the wave frequency). These conditions are applicable both to electromagnetic and gravitational waves. The condition for diffraction is more easily fulfilled for gravitational waves than for electromagnetic waves, since the wavelength is much bigger for GWs (in stellar-mass compact binary mergers at least, $\lambda \sim 10^2 - 10^4$ km). Furthermore, GWs experience nearly no absorption, unlike electromagnetic waves (which get partially or fully absorbed by interstellar gas and dust), so we receive them nearly neat, only distorted by possible gravitational lensing on their way.

An important length scale is the Einstein radius, $R_E = \sqrt{2R_S\mathcal{D}}$, with $\mathcal{D} = d_L d_{LS}/d_S$ the so-called reduced or effective distance, where d_L is the observer-lens distance, d_S the observer-source distance and d_{LS} the lens-source one. For the case of interest we assume $d_L \ll d_{LS}$. Lensing effects are expected to be significant when the source, lens and observer are aligned within approximately the angle $\theta_E = R_E/d_L$, called Einstein angle. As we can see in Fig. 3, for a circularly symmetric lens, the angles are related as $\beta = \theta - \alpha(\theta)$, which is called the *lens equation*.

IV. POINT MASS LENS

There are several models of lens, depending on the size, mass and density profile of the lensing mass distribution. We will consider a *point mass lens* model. The corresponding physical object could be a compact object (BH, NS) or a massive star.

For this model, the virtual image positions are [5]

$$\theta_\pm = \frac{\beta}{2} \pm \frac{1}{2}\sqrt{\beta^2 + 4\theta_E^2}. \tag{8}$$

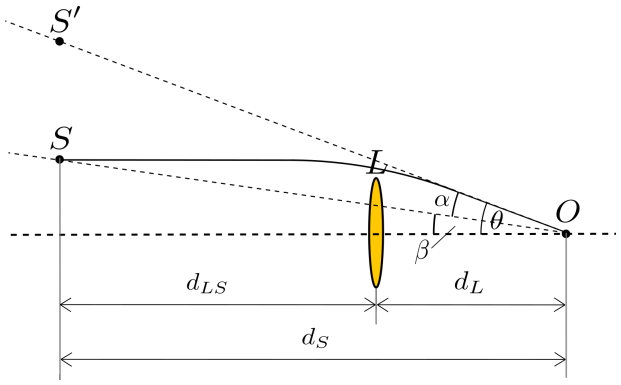

FIG. 3: Qualitatively general configuration of a circularly symmetric gravitational lens (L). The observer, at O, sees the virtual source S' at an angle θ, but the real source S is in fact further away and at a different angle, β. The difference between these two angles is the reduced deflection angle α. The wave propagation follows the solid line path. The horizontal dashed line represents the optical axis. In the thin lens approximation, the piece of path where the light is curved should be much smaller than the total distance travelled.

That means we have two virtual images.

For small angles, the point mass lens gravity effects can be treated analogously to having an index of refraction. From the wave equation, and assuming $h = \psi(R)e^{i\omega t}$ (where h is the GWs field, $\psi(R)$ is the the amplitude of the wave and $\omega = 2\pi f$ the angular frequency of the gravitational wave), the wave equation in the weak field limit can be written as a scalar wave equation [6]

$$\nabla^2\psi + \left(k^2 + \frac{2\varkappa k}{r}\right)\psi = 0, \tag{9}$$

where $\varkappa = 4\pi G M_L f/c^3$ with $k = 2\pi f/c$ (the wave number), and r the distance to the lens. It turns out that this wave equation is analogous to the time-independent Schrödinger equation for Coulomb scattering [6]. This means that the wave propagation will follow the same paths that charged particles would follow in a scattering experiment (at the lowest order) with an attracting Coulomb force. Here, $\varkappa = R_S/\lambda$, so $\varkappa$ is an indicator of the regime where we are working (discussed in Sec. III). This is valid for both electromagnetic and gravitational waves.

The solution for Eq.(9) was found by W. Gordon in 1928 in an exact analytical form [7]

$$\psi(f) = e^{ikr\cos\theta} e^{\pi\varkappa/2}\Gamma(1 - i\varkappa)\, {}_1F_1(i\varkappa, 1; 2ikr\sin^2(\theta/2)), \tag{10}$$

composed of the gamma function Γ, the confluent hypergeometric function ${}_1F_1$ and exponentials. r and θ are the spherical coordinates, with the optical axis as the z-axis and the lens at the origin.

In our case we consider a gravitational field, unlike the electrostatic field in the scattering, so the charges are replaced by masses (as the sources of the field). It's interesting that both systems can be treated the same way since they are different fields.

V. AMPLIFICATION FACTOR

The lensed image is distorted and magnified, so the amplitude and phase of the received wave are different than what they would be without lens. The amplification factor is defined as the wave amplitudes ratio [8]:

$$F(f) = \frac{\psi(f)}{\psi_0(f)}, \tag{11}$$

where $\psi(f)$ and $\psi_0(f)$ are the amplitude of the lensed and unlensed (if there was no lens) waves, respectively.

For a point mass lens, if the deflection zone is much smaller than the total distance travelled (thin lens approximation), the amplification factor is [7–9]

$$F(f) = \exp\left\{\frac{\pi}{2}\varkappa + i\varkappa\left[\ln(\varkappa) - 2\phi_m(y)\right]\right\} \times \Gamma(1 - i\varkappa)\, {}_1F_1(i\varkappa, 1; i\varkappa y^2), \tag{12}$$

which comes from Eq.(10). Here, $\phi_m(y) \equiv (x_m - y)^2/2 - \ln(x_m)$, where $x_m \equiv (y + \sqrt{y^2+4})/2$, being $y = \theta/\theta_E$ the normalised angle [8–10]. We can see its absolute value $|F|$ in Fig. 4, as a function of two variables: y and f. We introduce τ_d, the normalised delay time, $\tau_d = \Delta t/(4GM_L/c^3)$, where Δt is defined as the delay time, the difference in time between the different images. For a point mass lens, its expression is $\tau_d = y\sqrt{y^2+4}/2 + \ln\{[\sqrt{y^2+4}+y]/[\sqrt{y^2+4}-y]\}$ [8] with two contributions: the difference in path length, and the slowing of time near massive objects. For a fixed y and varying $f\tau_d$ (these would correspond to a change in frequency from a slowly moving source, for example), $|F|$ oscillates with the same amplitude, which increases when we approach $y = 0$. In $y = 0$ it grows exponentially, as we will see. For a fixed f (which would correspond to a monochromatic source moving perpendicular to the optical axis, thus changing y), there are also oscillations with varying amplitude, peaking in $y = 0$. The oscillations are due to the interference of waves coming from two images

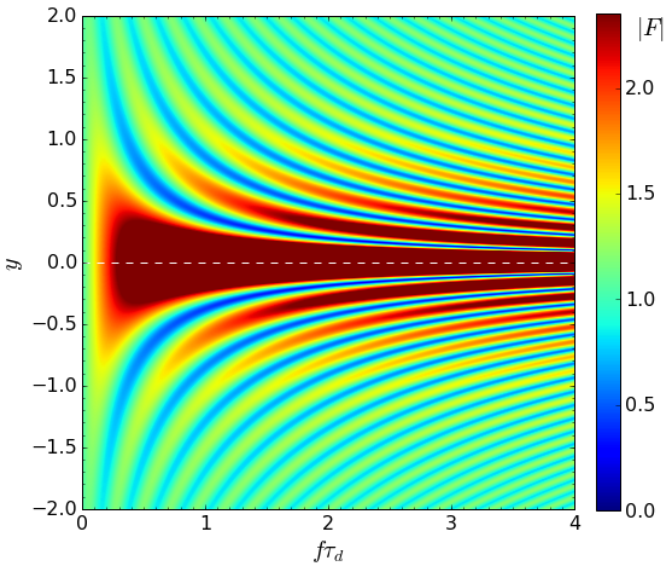

FIG. 4: Colour map of the absolute value of the amplification factor $|F|$ for a point mass lens. The normalised angle $y = \theta/\theta_E$ is represented in the y axis, and the normalised frequency (τ_d being the delay time and f the GWs frequency) in the x axis. Along the line of sight ($y = 0$), $|F|$ has the largest values, and moving along each axis, there are oscillating patterns due to interference.

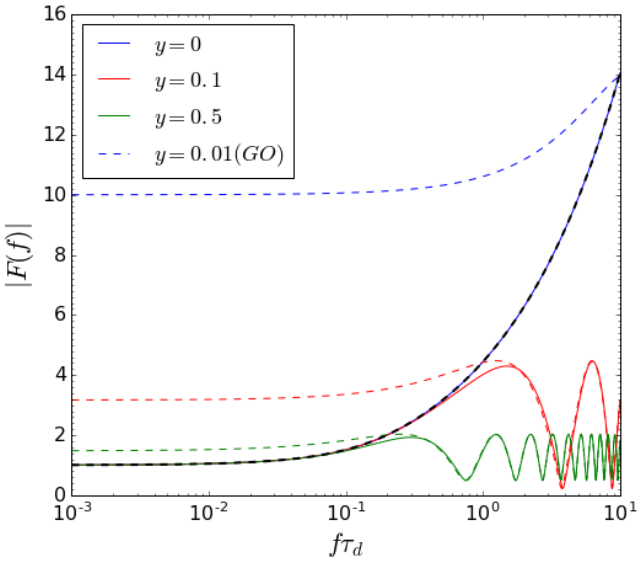

FIG. 5: Absolute value of the amplification factor for different angles y, as a function of the normalised frequency. These are sections of fixed y of Fig. 4. Solid lines correspond to the exact result and dashed lines to GO approximation, for different y: each one represented by the same colour. We can't draw a $y = 0$ GO line ($|F(f)|$ diverges), instead we take $y = 0.01$ to see the comparison. The black dashed line corresponds to the asymptotic result for $y = 0$ (Eq.(13)). We can see that for high frequencies, GO is a good approximation, but not for $f \lesssim \tau_d^{-1}$. These results agree with those obtained by other authors [8],[9].

In Fig. 5 we plot $|F|$ as a function of the frequency f for several fixed values of the angle y. We can see that the GO approximation is good if $f \gg \tau_d^{-1}$. It is for $f \lesssim \tau_d^{-1}$ that wave effects need to be taken into account. The smaller y, the bigger the deviation in $|F(f)|$ from the exact result. For small f, all curves converge to an asymptotic line (the square root of the maximum magnification μ_{max} [9]):

$$|F(y=0)|^2 = \mu_{max} = \frac{2\pi^2 f}{1 - e^{-2\pi^2 f}}. \tag{13}$$

In Fig. 6 we plot $|F|$ as a function of the angle y for several fixed values of the frequency f. The figure shows that for $f \gg \tau_d^{-1}$ there are more oscillations and the peak is higher, whereas for $f \ll \tau_d^{-1}$ it's the other way around, it can even have only one oscillation. In GO, these last

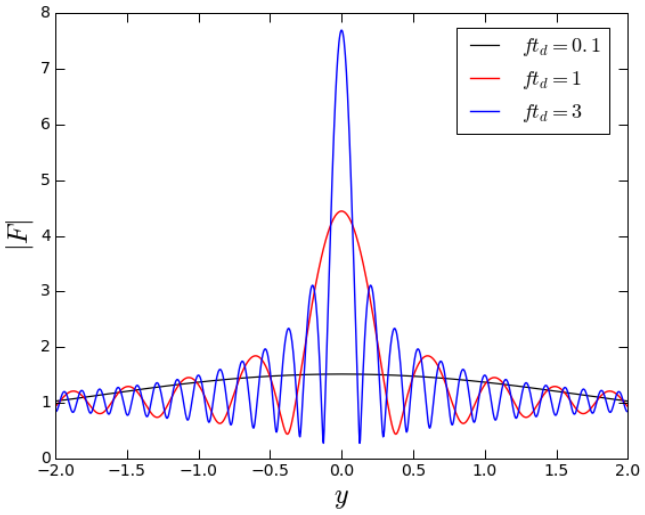

FIG. 6: Absolute value of the amplification factor for different $f\tau_d$, as a function of the angle y. These are sections of fixed $f\tau_d$ of Fig. 4. All cases have a peak at $y = 0$ and have decreasing oscillations (the number of which also depends on $f\tau_d$) as $|y|$ increases.

case would have an infinite peak at $y = 0$, far from the exact result.

VI. CONCLUSIONS

We have analysed the expression of the Fourier transform of the "chirp" from the gravitational waves generated in binary systems. We have obtained an analytic expression for it with the stationary phase approximation and its improved expression. For our purpose of identifying variations due to gravitational lensing, it would be convenient to search for a signal with a longer time interval to reduce finite time effects. So, knowing some of the recent detections, these would correspond to lower mass compact binaries (NS) whose inspiral lasts longer.

Once the GWs propagate, they can encounter distributions of mass with $M_L \lesssim 10^5(M_\odot/f)$ Hz, which can lens the GWs and produce wave effects. For a *point mass lens* model, the wave deviates the same way as Coulomb scattered particles. Depending on the angle y , the frequency f and the distance, the lensing effect is different. We have analysed the absolute value of the amplification factor $|F(f)|$, and we have seen that wave effects are manifested in the modulation of the wave amplitude, which is a function of the angle of observation and of the frequency.

To sum up, wave effects are important when the wavelength of the gravitational wave is of the same order as the Schwarzschild radius of the binary system, and need to be taken into account.

Knowing the chirp waveform and the amplification factor expression, the next step would be to obtain a gravitationally lensed chirp expression from a compact binary merger by doing a Fourier transform of the product of the unlensed waveform and the amplification factor.

Acknowledgments

This work has only been possible with the advice, support and dedication of my advisor Oleg Bulashenko. I would like to thank him for all his time, to talk and discuss everything. I would also like to thank my parents and my brother for having encouraged me and listened to me during all my career. And to all my good companions in this journey.

[1] P. Schneider, J. Ehlers and E.E. Falco, *Gravitational Lenses*, (Springer-Verlag, Berlin, 1992)

[2] Charles W. Misner, Kip S. Thorne, John Archibald Wheeler, *Gravitation*, (W.H. Freeman Company, San Francisco, 1973)

[3] Michele Maggiore, *Gravitational Waves. Theory and Experiments*, Vol.1. (Oxford University Press Inc., New York, 2008)

[4] Damour, Thibault and Iyer, Bala R. and Sathyaprakash, B.S.. "Frequency-domain P-approximant filters for time-truncated inspiral gravitational wave signals from compact binaries". Phys. Rev. D. **62**: 084036 (2000)

[5] Narayan, Ramesh and Bartelmann, Matthias. "Lectures on Gravitational Lensing". Jerusalem Winter School, Cambridge University Press (1995)

[6] Deguchi, Shuji and Watson, William D.."Diffraction in Gravitational Lensing for Compact Objects of Low Mass". Ap.J. **307**: 30-37 (1986)

[7] Gordon, W.. "Über den Stoss zweier Punktladungen nach der Wellenmechanik". Zeitschrift für Physik. **48**: 180-191 (1928)

[8] Takahashi, Ryuichi and Nakamura, Takashi. "Wave Effects in the Gravitational Lensing of Gravitational Waves from Chirping Binaries". Ap.J. **595**: 1039-1051 (2003)

[9] Matsunaga, Norihito and Yamamoto, Kazuhiro. "The finite source size effect and wave optics in gravitational lensing". Journal of Cosmology and Astroparticle Physics **2006 01**: 023 (2006)

[10] Nakamura, Takahiro T.. "Gravitational Lensing of Gravitational Waves from Inspiraling Binaries by a Point Mass Lens". Phys. Rev. Lett. **80**: 1138-1141 (1998)